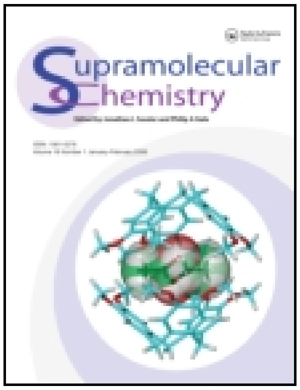

Supramolecular Chemistry
Publication details, including instructions for authors and subscription information:
http://www.tandfonline.com/loi/gsch20

Theoretical studies on the electronic structure of the synthetic complex of soluble methanemonooxygenase intermediate Q

Toru Saito [a], Yusuke Kataoka [a], Yasuyuki Nakanishi [a], Yasutaka Kitagawa [a], Takashi Kawakami [a], Shusuke Yamanaka [a], Mitsutaka Okumura [a] & Kizashi Yamaguchi [a]

[a] Department of Chemistry, Graduate School of Science, Osaka University, 1-1 Machikaneyama, Toyonaka, Osaka, 560-0043, Japan

To cite this article: Toru Saito, Yusuke Kataoka, Yasuyuki Nakanishi, Yasutaka Kitagawa, Takashi Kawakami, Shusuke Yamanaka, Mitsutaka Okumura & Kizashi Yamaguchi (2011): Theoretical studies on the electronic structure of the synthetic complex of soluble methanemonooxygenase intermediate Q, Supramolecular Chemistry, 23:01-02, 83-87

To link to this article: http://dx.doi.org/10.1080/10610278.2010.510560

Supramolecular Chemistry
Vol. 23, Nos. 1–2, January–February 2011, 83–87

Theoretical studies on the electronic structure of the synthetic complex of soluble methanemonooxygenase intermediate Q

Toru Saito*, Yusuke Kataoka, Yasuyuki Nakanishi, Yasutaka Kitagawa, Takashi Kawakami, Shusuke Yamanaka, Mitsutaka Okumura and Kizashi Yamaguchi

Department of Chemistry, Graduate School of Science, Osaka University, 1-1 Machikaneyama, Toyonaka, Osaka 560-0043, Japan

(*Received 10 June 2010; final version received 20 July 2010*)

We investigate for the first time the electronic structure of the biomimetic diiron complex **1** $[Fe(IV)_2(\mu\text{-}O)_2(5\text{-}Me_3\text{-}TPA)_2]^{4+}$ (5-Me$_3$-TPA = tris(5-methyl-2-pyridylmethyl)amine) using broken-symmetry hybrid density functional theory method. According to previous studies, the $Fe(IV)_2(\mu\text{-}O)_2$ core of intermediate Q of soluble methane monooxygenase shows antiferromagnetic coupling between local $S = 2$ states at each iron site. In contrast to Q, each local Fe(IV) ion of the synthetic complex does not have an $S = 2$ but has an $S = 1$ state based on the calculated geometric parameters and energetic stability. Our calculation supports the experimental result.

Keywords: DFT; Fe_2O_2; MMO; magnetic coupling constant

The soluble methane monooxygenase (sMMO) catalyses the conversion of methane to methanol by activating dioxygen (*1*). According to spectroscopic studies, the high reactive intermediate (Q) is assumed to have the $Fe(IV)_2(\mu\text{-}O)_2$ diamond core (*2*). The intermediate Q has been considered as a key intermediate that undergoes hydroxylation of methane. The Mössbauer study showed that two Fe(IV) sites are antiferromagnetically (AF) coupled ($J < -30\,\text{cm}^{-1}$), indicating that the ground state is $S_{\text{tot}} = 0$ (*3*). The EXAFS spectra suggested that the $Fe(IV)_2(\mu\text{-}O)_2$ core has one short (1.77 Å) and one long (2.05 Å) Fe—O bond. Although both Fe sites are in an oxidation state of IV, the electronic configuration is still an open question whether each Fe(IV) has an intermediate spin (IS, $S = 1$) $^1[Fe(IV)(S = 1)(O^{2-})_2Fe(IV)(S = -1)]$ (**a**) or a high spin (HS, $S = 2$) $^1[Fe(IV)(S = 2)(O2)_2Fe(IV)(S = -2)]$ (**b**) state. Several theoretical studies investigated the possible spin states of Q by using broken-symmetry (BS) hybrid density functional theory (DFT) approach (*4*, *5*). These studies concluded that (**b**) is more reliable because (**a**) is found to be 7.5 kcal/mol higher than (**b**).

Very recently, Que and co-workers (*6*) reported the synthetic complexes, which have the $Fe(IV)_2(\mu\text{-}O)_2$ diamond core, namely $[Fe(IV)_2(\mu\text{-}O)_2(5\text{-}Me_3\text{-}TPA)_2]^{4+}$ (**1**) (5-Me$_3$-TPA = tris(5-methyl-2-pyridylmethyl)amine) and $[Fe(IV)_2(\mu\text{-}O)_2(L)_2]^{4+}$ (**2**) (L = tris(3,5-dimethyl-4-methoxypyridyl-2-methyl)amine). Compound **2** is quite stable as compared to **1**, which has a high self-decay rate. At present, this is the only synthetic complex proposed for Q. According to Mössbauer spectroscopy and EXAFS data, two Fe(IV) ions are AF coupled ($J < -40\,\text{cm}^{-1}$), and the Fe—Fe distance is 2.73 Å. In contrast to Q, the electronic configuration (**a**) was assumed to be reasonable. Since there is no X-ray crystallographic data, the detail is still unclear. The goal of the present study is to determine whether (**a**) is the ground state from a viewpoint of computational calculation. We compare the geometric parameters and the magnetic coupling constant values between calculations and the experiment. To our knowledge, it is the first attempt to examine the geometric and electronic structure of such complex.

Since there is no X-ray structure, the initial structure of the present model was constructed based on the complex $[Fe(IV)_2(\mu\text{-}O)(OH)O(L)_2]^{3+}$ (L = tris(3,5-dimethyl-4-methoxypyridyl-2-methyl)amine) reported by Martinho et al. (*7*). We investigate **1** instead of **2** for simplicity as depicted in Figure 1.

The magnetic properties of transition metal complexes are usually predicted with the use of Heisenberg Hamiltonian. In the present study, we used a two-spin Heisenberg model approximation,

$$\hat{H} = -2JS_{\text{Fe1}}.S_{\text{Fe2}}, \qquad (1)$$

where S_{Fe1} and S_{Fe2} represent spin operators at sites Fe1 and Fe2, respectively. J is an effective exchange integral. Based on this notation, (**a**) and (**b**) represent $S_{\text{Fe1}} = -S_{\text{Fe2}} = 1$ and $S_{\text{Fe1}} = -S_{\text{Fe2}} = 2$, respectively. J can be determined by the computational method as well as by magnetic susceptibility. According to a recent computational development, a single-point energy calculation by high-level *ab initio* methods such as coupled cluster and

---

*Corresponding author. Email: tsaito@chem.sci.osaka-u.ac.jp

ISSN 1061-0278 print/ISSN 1029-0478 online

DOI: 10.1080/10610278.2010.510560
http://www.informaworld.com

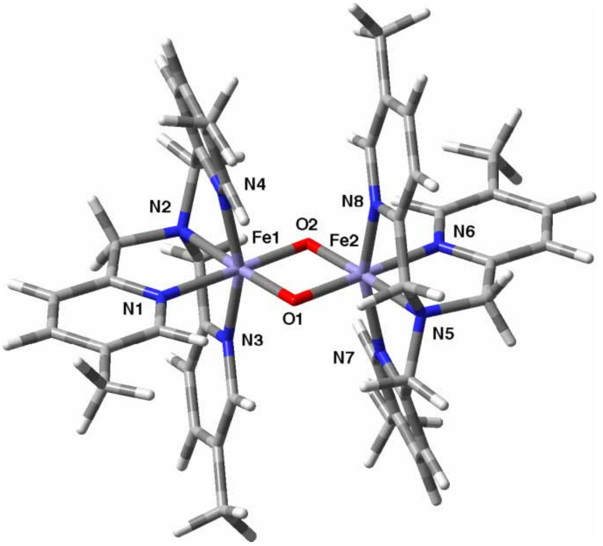

Figure 1. Calculated model $[Fe(IV)_2(\mu\text{-}O)(OH)O(5\text{-}Me_3\text{-}TPA)_2]^{4+}$(**1**) (5-$Me_3$-TPA = tris(5-methyl-2-pyridylmethyl)-amine).

Table 1. Optimised structural parameters[a] of (**a**) and (**b**) together with EXAFS data.

Parameters	Model (**a**)	Model (**b**)	Expt.[b]
Fe1—Fe2	2.74	2.68	2.73
O1—O2	2.34	2.38	
Fe1—O1	1.81	1.80	1.77[c]
Fe1—O2	1.79	1.78	
Fe2—O1	1.81	1.78	
Fe2—O2	1.80	1.80	
∠ Fe1—O1—Fe2	98.3	96.6	101[c]
∠ Fe1—O2—Fe2	99.6	96.7	
Fe1—N1	2.03	2.02	1.96[c]
Fe1—N2	2.07	2.14	
Fe1—N3	2.00	2.21	
Fe1—N4	2.00	2.21	
Fe2—N5	2.05	2.14	
Fe2—N6	2.00	2.01	
Fe2—N7	2.01	2.21	
Fe2—N8	2.01	2.21	

[a] Bond lengths, in Å; angles, in deg.
[b] From Ref. (*6*).
[c] The average value.

multi-reference methods can be performed for small chemical systems. However, calculations using these methods are computationally expensive and it is impossible to apply them to larger systems. Instead, BS DFT calculations are suggested to give an alternative way at lower computational costs with both dynamical and non-dynamical electron correlation corrections. The BS DFT approach is a 'de facto standard' for calculating electronic structures of transition metal complexes. It is well known, however, that the BS method has a fatal flaw called the spin contamination error. The energy of the BS ($S_{\mathrm{tot}} = 0$) state is estimated to be incorrect due to HS states. In order to eliminate the spin contamination error, Yamaguchi et al. proposed the approximate spin-projection (AP) procedure by using a simple approximation that the spin contamination in a high spin (HS) state is negligible (*8*). The corrected J value is

$$J = \frac{E^{\mathrm{BS}} - E^{\mathrm{HS}}}{\langle S^2\rangle^{\mathrm{HS}} - \langle S^2\rangle^{\mathrm{BS}}}, \tag{2}$$

where $E^{(x)}$ and $\langle S^2\rangle^{(X)}$ denote the total energy and the expectation value of total spin angular momentum for the spin state X, respectively. The corrected BS energy (AP) using the correct spin state is expressed as

$$E^{\mathrm{AP}} = E^{\mathrm{BS}} + J\langle S^2\rangle^{\mathrm{BS}}. \tag{3}$$

In this paper, the magnetic interaction between two Fe(IV) ions is discussed using Equation (2) by using the $S_{\mathrm{tot}} = 2$ ($S_{\mathrm{Fe1}} = S_{\mathrm{Fe2}} = 1$) and $S_{\mathrm{tot}} = 4$ ($S_{\mathrm{Fe1}} = S_{\mathrm{Fe2}} = 2$) states as the HS states corresponding to (**a**) and (**b**). All the calculations were performed by Gaussian 03 (*9*) at the UB3LYP level of theory (*10*). The geometry optimisations were performed for (**a**) and (**b**) together with MIDI + pd (53321/5321/411) basis sets (*11*, *12*) for Fe and 6-31G* basis sets for the other atoms.

First, we compare structural parameters between (**a**) and (**b**). The optimised structural parameters are summarised in Table 1 together with available EXAFS data measured at 10 K (*6*).

As listed in Table 1, the parameters of (**a**) are closer to the EXAFS data, indicating that each Fe(IV) ion has $S = 1$. The Fe—Fe distance of (**b**) (2.68 Å) is slightly shorter than the EXAFS data (2.73 Å), while that of (**a**) is in good agreement with it. The average value of the Fe—N distances also supports that (**a**) is more reliable than (**b**).

Next, computed Mulliken spin and charge populations on the Fe_2O_2 core of (**a**) and (**b**) are summarised in Table 2. The spin populations on two Fe atoms differ from their number of unpaired electrons (2 for (**a**) and 4 for (**b**)), suggesting the electron donations from the ligands. In fact, the obtained charge populations on the Fe atoms are slightly smaller than their formal value IV. The spin state of iron atoms for **1** differs from Q of sMMO in the ligand environment (*6*). In contrast to **1**, which has nitrogen-rich ligands, oxygen atoms of glutamic acids are also ligated in Q.

Calculated spin populations on the Fe_2O_2 core of (**a**) are not symmetric because of the asymmetric Fe_2O_2 core. On the other hand, the optimised Fe_2O_2 core of (**b**) is symmetric. As for Q, the slight asymmetric Fe_2O_2 core

Table 2. Mulliken spin and charge populations on the Fe_2O_2 core.

Model	Spin state	Mulliken spin (charge) population				Ref.
		Fe1	Fe2	O1	O2	
(a)	HS	1.84 (1.25)	1.59 (1.23)	0.40 (−0.68)	0.35 (−0.70)	This work
	BS	1.94 (1.26)	−1.70 (1.22)	−0.20 (−0.70)	−0.06 (−0.72)	This work
Q1[a]	BS	1.71	−1.52	−0.57	0.38	(*13*)
	BS	1.6	−1.7	−0.4	0.4	(*14*)
(b)	HS	3.32 (1.25)	3.32 (1.25)	0.35 (−0.74)	0.34 (−0.74)	This work
	BS	3.28 (1.24)	−3.28 (1.24)	0.02 (−0.72)	0.02 (−0.72)	This work
Q2[b]	HS	3.44	3.55	0.30	0.44	(*15*)
	BS	3.54	−3.49	−0.06	−0.03	(*16*)

[a] $S_{Fe1} = -S_{Fe2} = 1$.
[b] $S_{Fe1} = S_{Fe2} = 2$ for HS state and $S_{Fe1} = -S_{Fe2} = 2$ for BS state.

is favourable based on previous theoretical studies (*13–16*). This is attributed to the asymmetric ligand environment of Q. Since the ligand of **1** is more symmetric than Q, it is expected that both geometric and electronic structures of the Fe_2O_2 core are symmetric. However, the Fe1—O1—Fe2 angle and the Fe1—O2—Fe2 angle are not equivalent, leading to asymmetric spin populations on the Fe_2O_2 core. In our opinion, there are two reasons for this: (1) the asymmetric Fe_2O_2 core of (**a**) can result from the inadequate approximation. It is difficult to describe the on-site Coulomb repulsion and transfer integral properly at the BS DFT level. Nevertheless, the high-level *ab initio* methods cannot be applied to such a large system and (2) the present model is insufficient. In this study, we do not consider the effect of counterions $(ClO_4^-)_4$ in the model complex because there is no available information about them. The geometry of the Fe_2O_2 core can be variable due to the presence of the counterion because it affects the charge distribution (*17*). This will be discussed in the future work after the X-ray crystallographic structure is taken. The magnetic coupling constant (J) values between two Fe(IV) ions calculated by Equation (2) are summarised in Table 3. Total energies and expectation values of total spin angular momentum are also summarised in Table 3.

In this study, we used the $\langle S^2\rangle^{BS}$ value of the Kohn–Sham orbital that is expressed by the single Slater determinant for the non-interacting reference (Kohn–Sham) system.

$$\langle S^2\rangle^{BS} = \frac{N_\alpha - N_\beta}{2}\left(\frac{N_\alpha - N_\beta}{2} + 1\right) + N_\beta - \sum_i^N \sum_j^N \left|S_{ij}^{\alpha\beta}\right|^2. \tag{4}$$

The definition of $\langle S^2\rangle^{BS}$ (Equation (4)) indicates that when there is no interaction between two Fe(IV) ions, these values are 2.0 and 4.0. The obtained $\langle S^2\rangle^{BS}$ values are 1.9893 and 3.9269 for (**a**) and (**b**), respectively.

Calculated J values of (**a**) and (**b**) are −38 and −202 cm^{-1}, respectively. These values are comparable to the results of Q, i.e. −59 and −188 cm^{-1} (in our definition) for $S_{Fe1} = -S_{Fe2} = 1$ and $S_{Fe1} = -S_{Fe2} = 2$, respectively (*4*). In order to consider the orbital–orbital interaction, we performed natural orbital analysis for (**a**) and (**b**). Figures 2 and 3 depict bonding and antibonding NOs of the Fe_2O_2 core for (**a**) and (**b**) corresponding to magnetic orbitals together with orbital overlap (T_i) values given by their occupation numbers (n_i) of bonding NOs (*18*).

$$T_i = n_i - 1. \tag{5}$$

In the case of (**a**), the pair of the highest occupied NO − 1 (HONO − 1) and the lowest unoccupied NO (LUNO − 1)

Table 3. Calculated total energies,[a] $\langle S^2\rangle$ values and magnetic coupling constant (J) values[b] for (**a**) and (**b**).

Model	BS state		HS state			
	E^{BS}	$\langle S^2\rangle^{BS}$	E^{HS}	$\langle S^2\rangle^{HS}$	E^{AP}	J
(a)	−4743.5239	1.9893	−4743.5231	6.0744	−4743.5242	−38
(b)	−4743.5152	3.9269	−4743.5003	20.1352	−4743.5188	−202

[a] In a.u.
[b] In cm^{-1}.

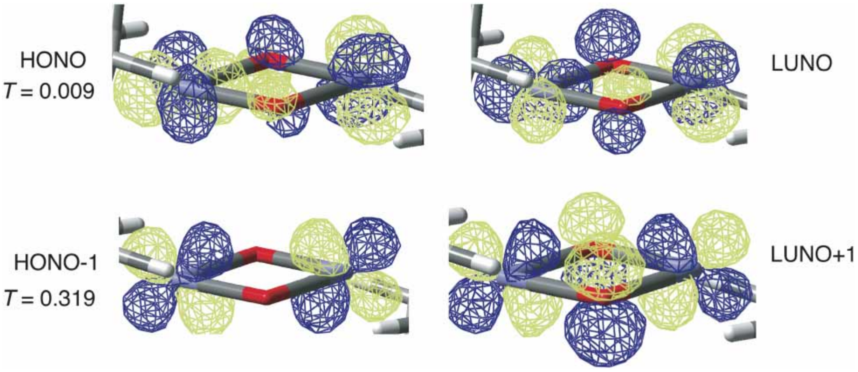

Figure 2. Natural orbitals of the Fe_2O_2 core corresponding to magnetic orbitals for (**a**).

represents a π-type interaction through bridging oxo, leading to the orbital overlap ($T = 0.319$). Martinho et al. (*7*) reported that two Fe spins ($S = 1$) in the [HO—Fe1(IV)-—O—Fe2(IV) = $O(L)_2]^{3+}$ are ferromagnetically coupled to yield the ground quintet ($S_{\mathrm{tot}} = 2$) state. According to their calculations, the J value was predicted to be $+160\,\mathrm{cm}^{-1}$ in our definition (see Equation (1)). They suggested that inequivalent coordinations at two Fe sites cause ferromagnetic interactions. On the other hand, looking at the HONO–LUNO pair, the bridging oxo in the diamond core of (**a**) provides the two Fe spins with weak orbital overlap ($T = 0.009$), although the $d_{x^2-y^2}$ of Fe1 and the d_{xz} of Fe2 are orthogonal. Therefore, (**a**) shows antiferromagnetic interaction consistent with its negative J value ($-38\,\mathrm{cm}^{-1}$). Although the obtained J values of (**a**) do not quantitatively agree with the experiment ($J < -40\,\mathrm{cm}^{-1}$), the corrected BS state (AP state) is more stable than the HS state by 0.7 kcal/mol, and the result supports the singlet ground state.

As for (**b**), the HONO $- X$–LUNO $- X\,(X = 3, 2, 1, 0)$ pair corresponds to δ_1, σ, π, and δ_2 interactions with relatively large T values in comparison with the

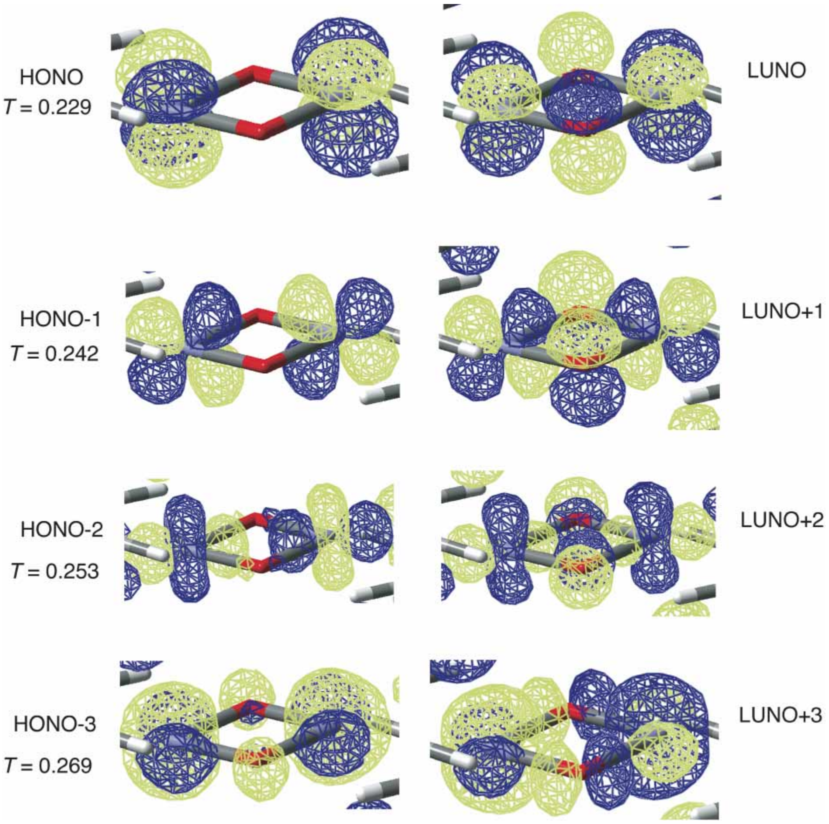

Figure 3. Natural orbitals of the Fe_2O_2 core corresponding to magnetic orbitals for (**b**).

HONO–LUNO pair of (**a**). The difference in J values between (**a**) and (**b**) reflects the strength of the orbital interactions. Finally, we compared the energy between (**a**) and (**b**). The total energy of (**a**) for the $S_{\mathrm{tot}} = 0$ state is lower than that of (**b**) by 3.4 and 5.5 kcal/mol with and without spin projection. The result also supports that (**a**) is a more likely candidate for the biomimetic diiron complex for Q.

In summary, we investigate the electronic structure of the diiron complex by using BS hybrid DFT method with the AP correction. According to previous studies, the $\mathrm{Fe(IV)_2(\mu\text{-}O)_2}$ core of intermediate Q of sMMO shows antiferromagnetic coupling between local $S = 2$ states at each iron site. On the other hand, based on the calculated results, each local Fe(IV) ion of the complex does not have an $S = 2$ but has an $S = 1$ state. The calculated J value shows antiferromagnetic interaction ($S_{\mathrm{tot}} = 0$). Since there is no information about the X-ray structure, our calculated results support the experimental spectroscopic data.

Acknowledgements

T.S. is grateful for the Research Fellowships from the Japan Society for the Promotion of Science for Young Scientists (JSPS). This work has been supported by Grants-in-Aid for Scientific Research (KAKENHI) (Nos. 19750046, 19350070) from JSPS and Grant-in-Aid for Scientific Research on Innovative Areas (No. 22108515) from the Ministry of Education, Culture, Sports, Science and Technology (MEXT).

References

(1) Merkx, M.; Kopp, D.A.; Sazinsky, M.H.; Blazyk, J.L.; Müller, J.; Lippard, S.J. *Angew. Chem., Int. Ed.* **2001**, *40*, 2782–2807.
(2) Shu, L.; Nesheim, J.C.; Kauffmann, K.; Münck, E.; Lipscomb, J.D.; Que, L., Jr. *Science* **1997**, *275*, 515–518.
(3) Lee, S.-K.; Fox, B.G.; Froland, W.A.; Lipscomb, J.D.; Münck, E. *J. Am. Chem. Soc.* **1993**, *115*, 6450–6451.
(4) Lovell, T.; Han, W.-G.; Liu, T.; Noodleman, L. *J. Am. Chem. Soc.* **2002**, *124*, 5890–5894.
(5) Baik, M.-H.; Newcomb, M.; Friesner, R.A.; Lippard, S.J. *Chem. Rev.* **2003**, *103*, 2385–2420.
(6) Xue, G.; Wang, D.; De Hont, R.; Fiedler, A.T.; Shan, X.; Münck, E.; Que, L., Jr. *Proc. Natl. Acad. Sci. USA* **2007**, *104*, 20713–20718.
(7) Martinho, M.; Xue, G.; Fiedler, A.T.; Que, L., Jr.; Bominaar, E.L.; Münck, E. *J. Am. Chem. Soc.* **2009**, *131*, 5823–5830.
(8) Yamaguchi, K.; Jensen, F.; Dorigo, A.; Houk, K.N. *Chem. Phys. Lett.* **1988**, *149*, 537–542.
(9) Frisch, M.J.; Trucks, G.W.; Schlegel, H.B.; Scuseria, G.E.; Robb, M.A.; Cheeseman, J.R.; Montgomery, J.A., Jr.; Vreven, T.; Kudin, K.N.; Burant, J.C.; Millam, J.M.; Iyengar, S.S.; Tomasi, J.; Barone, V.; Mennucci, B.; Cossi, M.; Scalmani, G.; Rega, N.; Petersson, G.A.; Nakatsuji, H.; Hada, M.; Ehara, M.; Toyota, K.; Fukuda, R.; Hasegawa, J.; Ishida, M.; Nakajima, T.; Honda, Y.; Kitao, O.; Nakai, H.; Klene, M.; Li, X.; Knox, J.E.; Hratchian, H.P.; Cross, J.B.; Adamo, C.; Jaramillo, J.; Gomperts, R.; Stratmann, R.E.; Yazyev, O.; Austin, A.J.; Cammi, R.; Pomelli, C.; Ochterski, J.W.; Ayala, P.Y.; Morokuma, K.; Voth, G.A.; Salvador, P.; Dannenberg, J.J.; Zakrzewski, V.G.; Dapprich, S.; Daniels, A.D.; Strain, M.C.; Farkas, O.; Malick, D.K.; Rabuck, A.D.; Raghavachari, K.; Foresman, J.B.; Ortiz, J.V.; Cui, Q.; Baboul, A.G.; Clifford, S.; Cioslowski, J.; Stefanov, B.B.; Liu, G.; Liashenko, A.; Piskorz, P.; Komaromi, I.; Martin, R.L.; Fox, D.J.; Keith, T.; Al-Laham, M.A.; Peng, C.Y.; Nanayakkara, A.; Challacombe, M.; Gill, P.M.W.; Johnson, B.; Chen, W.; Wong, M.W.; Gonzalez, C.; Pople, J.A. *Gaussian 03*; Revision E.01, Gaussian, Inc. Wallingford CT, 2004.
(10) Becke, A.D. *J. Chem. Phys.* **1993**, *98*, 5648–5652.
(11) Tatewaki, T.; Huzinaga, S. *J. Chem. Phys.* **1980**, *72*, 399–405.
(12) Hay, P.J. *J. Chem. Phys.* **1977**, *66*, 4377–4384.
(13) Siegbahn, P.E.M. *J. Biol. Inorg. Chem.* **2001**, *6*, 27–45.
(14) Yoshizawa, K.; Yumura, T. *Chem. Eur. J.* **2003**, *9*, 2347–2358.
(15) Basch, H.; Mogi, K.; Musaev, D.G.; Morokuma, K. *J. Am. Chem. Soc.* **1999**, *121*, 7249–7256.
(16) Gherman, B.F.; Dunietz, B.D.; Whittington, D.A.; Lippard, S.J.; Friesner, R.A. *J. Am. Chem. Soc.* **2001**, *123*, 3836–3837.
(17) Johansson, A.J.; Noack, H.; Siegbahn, P.E.M.; Xue, G.; Que, L., Jr *Dalton Trans.* **2009**, 6741–6750.
(18) Saito, T.; Kataoka, Y.; Nakanishi, Y.; Matsui, T.; Kitagawa, Y.; Kawakami, T.; Okumura, M.; Yamaguchi, K. *Chem. Phys.* **2010**, *368*, 1–6.